Dimeric Structure of the Six-Domain VibF Subunit of Vibriobactin Synthetase: Mutant Domain Activity Regain and Ultracentrifugation Studies†

Nathan J. Hillson and Christopher T. Walsh*

Department of Biological Chemistry and Molecular Pharmacology, Harvard Medical School, Boston, Massachusetts 02115

Received September 26, 2002; Revised Manuscript Received November 7, 2002

ABSTRACT: Nonribosomal peptide synthetases (NRPS), fatty acid synthases (FAS), and polyketide sythases (PKS) are multimodular enzymatic assembly lines utilized in natural product biosynthesis. Previous data on FAS and PKS subunits have indicated that they are homodimers and that some of their catalytic functions can work in trans. When NRPS assembly lines have been probed for comparable formation of stable oligomers, no evidence had been forthcoming that species other than monomer forms were active. In this work we focus on the six-domain (Cy1-Cy2-A-C1-PCP-C2) enzyme VibF from the vibriobactin synthetase assembly line, which contains three other proteins, VibB, VibE, and VibH, that—when purified and mixed with VibF and the substrates ATP, threonine, 2,3-dihydroxybenzoate (DHB), and norspermidine—produce the iron chelator vibriobactin. Using a deletion of the Cy1 domain and separate inactivating mutations in the Cy2, A, PCP, and C2 domains of VibF, we report regain of catalytic activity upon mutant protein mixing that argues for heterodimer formation, stable for hundreds to thousands of catalytic cycles, with acyl chain processing and transfer around blocked domains. Ultracentrifugation data likewise confirm a dimeric structure for VibF and establish that domains within NRPS dimeric modules can act on acyl chains in trans. The results described here are the first indication for an NRPS subunit that homodimerization can occur and that there is a continuum of functional oligomerization states between monomers and dimers in nonribosomal peptide synthetases.

Nonribosomal peptide (NRP),[1] fatty acid (FA), and many polyketide (PK) natural products are biosynthesized on multimodular enzymatic assembly lines (*1*−*3*). Each module has a set of catalytic domains, one carrier protein domain for recognition of an amino acid (NRP) or an acyl CoA monomer (PK), and subsequent covalent loading of the activated monomer unit in thioester linkage to a pantetheinyl prosthetic group attached to the carrier protein domain. The NRP or PK chains then grow as an elongating cascade of acyl-S-enzyme intermediates sequentially transferred to downstream modules through the pantetheinyl covalent tethers. There are core domains in any nonribosomal peptide synthetase (NRPS) module for activation (A) and condensation (C) functions along with the peptidyl carrier protein domain (PCP). Analogously, in a polyketide synthetase (PKS) module the acyltransferase domain (AT) covalently loads the holo acyl carrier protein domain (ACP), and the ketosynthase (KS) carries out the chain elongation C−C bond-forming step. There can be additional domains for epimerization (E) of amino acid chirality in NRPS modules, or for reduction (KR), dehydration (DH), and enoyl reduction (ER) in PKS modules. The presence of those extra domains determines the extent of chemical transformations that occur within the module before the chain transits to the next downstream module and sequential monomer addition. The order of modules and the inventory of core and optional domains provide the template for the specific sequence of the growing peptidyl and polyketidyl chains in these enzymatic assembly lines (Figure 1A).

The assembly lines must be arranged for efficient transfer of the covalently tethered acyl chains from one module to the next in each cycle of chain growth, both with regard to rates of chain transfer by the C or the KS domains, respectively, and with regard to yield, e.g., by sequestration of the activated thioesters from hydrolytic derailment. Some assembly lines, e.g., that for fatty acid synthases (FAS) (*1*), are accommodated within one large polypeptide, while others are distributed over multiple subunits, for example, three in deoxyerythronolide synthase (*2*) and three in vancomycin and tyrocidine synthetases (*3*, *4*), indicating requirements for protein−protein recognition for growing acyl chain transfer across subunit interfaces.

The nature of the oligomeric structure of FAS, PKS, and NRPS assembly line enzymes has been a topic of interest since quaternary structural arrangements could permit alternate paths of chain elongation. FAS and the deoxyerythro-

† This work has been supported by the National Institutes of Health (Grant AI42738 to C.T.W.). N.J.H. is funded by a National Defense Science and Engineering (NDSEG) fellowship.

* To whom correspondence should be addressed: phone 617-432-1715; fax 617-432-0438; e-mail christopher_walsh@hms.harvard.edu.

[1] Abbreviations: A, adenylation domain; ACP, acyl carrier protein; ArCP, aryl carrier protein; AT, acyl transferase domain; C, condensation domain; Cy, heterocyclization domain; DEBS, 6-deoxyerythronolide B synthase; DH, dehydrase domain; DHB, 2,3-dihydroxybenzoate; DHP, 2,3-dihydroxyphenyl; DTT, dithiothreitol; E, epimerization domain; ER, enoyl reductase domain; FAS, fatty acid synthase; ICL, isochorismate lyase; KR, β-ketoacyl reductase domain; KS, β-ketoacyl synthase domain; MAT, malonyl/acetyl transferase domain; mOx, 5-methyloxazoline; NRPS, nonribosomal peptide synthetase; PCP, peptidyl carrier protein; PKS, polyketide synthase; PP_i, inorganic pyrophosphate; TE, thioesterase domain.

10.1021/bi026903h CCC: $25.00
Published on Web 12/31/2002

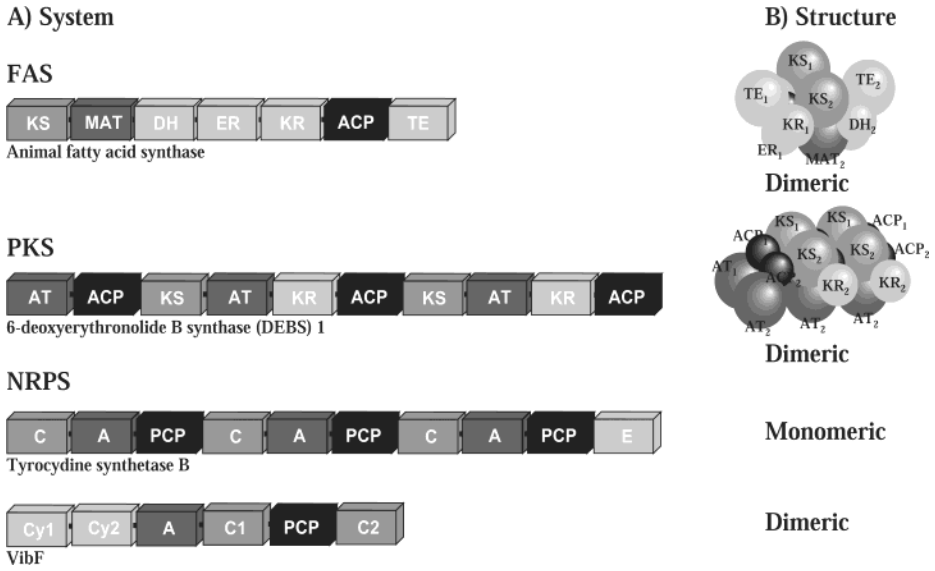

FIGURE 1: FAS, PKS, and NRPS assembly lines. (A) Linear domain layouts of representative synthases (FAS and PKS) and synthetases (NRPS). Domain abbreviations are as described in the text. (B) Predicted quaternary structures of the systems (*2*, *9*, *24*). Domain subscript numbering corresponds to one of the two parent peptide chains.

nolide B synthase PKS subunits have been shown to be dimers and the dimer state is required for activity (*5*, *6*). FAS dimers could be spontaneously dissociated by controlling salt concentrations at 4 °C, allowing for the reconstitution of heterodimers from inactive homodimeric mutants (*7*). Such spontaneous dissociation has not been observed for PKS dimers, but for both FAS and PKS systems, anion-exchange chromatography has served as a method for rapidly scrambling the dimer pair partners (*7*, *8*). Some heterodimers regained activity (*7*, *8*), leading to the view that some catalytic domains in an FAS or PKS module could act in trans on the domain in the paired module of the dimer. In addition to providing architectural constraints on the arrangement of domains within PKS and FAS modules, these results suggested the acyl chains could be transferred both in cis and in trans during elongation cycles.

In contrast, no evidence for homooligomeric organization of NRPS assembly lines has been forthcoming. In a recent study on modules from tyrocidine synthetase and enterobactin synthetase, evidence in favor of active monomeric modules was obtained by a combination of physical methods such as ultracentrifugation and genetic methods such as mutant complementation (*9*). To further probe the biochemistry of NRPS assembly lines we have been investigating NRPS for siderophore assembly, including pyochelin from *Pseudomonas aeruginosa* (*10*, *11*), yersiniabactin from *Yersinia pestis* (*12*), and vibriobactin from *Vibrio cholerae* (*13*, *14*). In this work we focus on the six-domain enzyme VibF from the vibriobactin synthetase assembly line, which contains three other proteins, VibB, VibE, and VibH, that—when purified and mixed with VibF and the substrates ATP, threonine, 2,3-dihydroxybenzoate (DHB), and norspermidine—produce the iron chelator vibriobactin (compound **2**). Vibriobactin is elaborated in microenvironments restricted in ferric iron. The siderophore is exported, complexes with Fe^{III} with remarkable affinity, and is imported back into the *V. cholerae* cell. The ability to produce the siderophore enhances the virulence of *V. cholerae*, the causative agent of cholera, in vertebrate infections (*15*, *16*).

Given the ability to reconstitute the full 10-domain assembly line and detect several intermediates, both bound as acyl-S-PCP (VibF) intermediates and soluble mono- and diacyl derivatives of DHB-spermidine (*13*, *14*), we have assigned functions to the six domains of VibF (Cy1-Cy2-A-C1-PCP-C2; Figure 1A), where Cy designates a variant of a condensation (C) domain that both condenses and cyclodehydrates DHB-threonyl moieties to yield the dihydroxyphenyl-methyloxazoline (DHP-mOx) rings that are characteristic of the vibriobactin siderophore structure (*14*). Using a deletion of the Cy1 domain and separate mutants in the Cy2, A, PCP, and C2 domains of VibF that individually lead to loss of catalytic activity, we report regain of catalytic activity upon mutant protein mixing that argues for heterodimer formation and acyl chain processing and transfer around the blocked domains. Ultracentrifugation data likewise confirm a dimeric structure for VibF and establish that domains within NRPS dimeric modules can act on acyl chains in trans.

EXPERIMENTAL PROCEDURES

Materials and General Methods. 2,3-DHB, coenzyme A, and all amino acids were purchased from Sigma−Aldrich Chemical Co. ATP was purchased from Boehringer Mannheim. TCEP was purchased from Fluka. DHP-mOx-spermidine-DHB was obtained as described previously (*17*). Standard recombinant DNA techniques and microbiological procedures were performed as described (*18*). Restriction enzymes and T4 DNA ligase were purchased from New England Biolabs. Pfu polymerase and competent *E. coli* were purchased from Stratagene. Oligonucleotide primers were purchased from Integrated DNA Technologies, and DNA sequencing to verify the fidelity of amplification was performed on double-stranded DNA by the Molecular Biology Core Facilities of the Dana Farber Cancer Institute (Boston, MA). Ni−NTA Superflow resin was purchased from Qiagen.

Design and Purification of VibF mutants. All mutations intended to eliminate the activity of single domains within

Chart 1

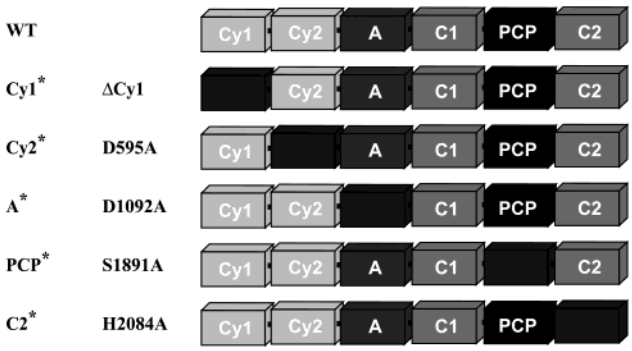

VibF (Chart 1) were as developed previously (*14*, *17*), with the exception of the A-domain mutation (hereafter denoted by A*) D1092A. This particular mutation was chosen so as to disrupt the essential aspartate residue (*19*), identified by alignment with the gramicidin S synthetase PheA. To concurrently eliminate the activity of multiple domains within VibF, single-domain mutations were concatenated [e.g., Cy2*PCP* contains the Cy2 domain mutation (Cy2*) D595A and the PCP domain mutation (PCP*) S1891A]. Mutants were purified as previously described (*14*).

Assay of VibF. Substrate-dependent ATP−PP_i exchange assays (100 μL) containing 10 nM VibF were performed as described previously (*13*). Three-minute secondary aminoacylation assays (25 μL) containing 200 nM holo-VibF were performed at 30 °C and analyzed by HPLC as described previously (*14*). The VibF mutant secondary aminoacylation complementation assays contained 100 nM of each mutant, and the mutant pairs were premixed for 1 h at 30 °C (during the generation of holo-VibF) before assay. For the time course of activity regain assays, the mutant pairs were premixed at either 30 or 4 °C after the generation of holo-VibF for the indicated amount of time before assay. For the concentration dependence/titration experiments, the concentrations of VibF were as indicated in the Results section.

Exponential Equilibration Model. The exponential equilibration model, utilized in fitting the time course for regain of catalytic activity experiments, assumes that the rate of heterologous dimer formation is proportional to the difference between the current and equilibrium concentrations of the heterologous dimer. Let A and B represent the two VibF mutants, and use the notation A·B and B·A for the heterologous dimers with A in the first and second dimer slot (respectively). For the premixing time experiment at 30 °C, the model results in

$$\text{rate} = \frac{2k_{\text{cat}[\text{A}\cdot\text{B}]}[\text{A}\cdot\text{B}]_{\text{eq}}}{[\text{A}]_0 + [\text{B}]_0}\left[1 - \frac{\tau}{\Delta t}\exp(-t/\tau)(1 - \exp(-\Delta t/\tau))\right]$$

where $k_{\text{cat}[\text{A}\cdot\text{B}]}$ is the catalytic rate of the dimeric pair A·B, defined by the activity divided by the concentration of A·B, $[\text{A}\cdot\text{B}]_{\text{eq}}$ is the equilibrium concentration of A·B (or equivalently B·A) at 30 °C, $[\text{A}]_0$ and $[\text{B}]_0$ are the total concentrations of A and B (respectively), τ is the characteristic time of mixing at 30 °C, Δt is the duration of the activity assay, and t is the premixing time at 30 °C. The definition of rate used here is the same as that used in Table 2 (the rate of vibriobactin production divided by the total VibF concentration), and the rate is the integral average over the course of the assay (as mixing occurs during the assay itself and must be accounted for). The model for premixing at 4 °C yields

Scheme 1

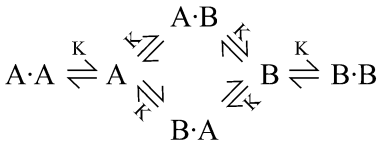

$$\text{rate} = \frac{2k_{\text{cat}[\text{A}\cdot\text{B}]}[\text{A}\cdot\text{B}]_{\text{eq}}}{[\text{A}]_0 + [\text{B}]_0}\left[1 - \frac{\tau}{\Delta t}\left[1 - \exp(-\Delta t/\tau) \times \left[1 - \frac{[\text{A}\cdot\text{B}]_{\text{eq}}^{4^\circ\text{C}}}{[\text{A}\cdot\text{B}]_{\text{eq}}}(1 - \exp(-t_{4^\circ\text{C}}/\tau_{4^\circ\text{C}}))\right]\right]\right]$$

where $[\text{A}\cdot\text{B}]_{\text{eq}}^{4^\circ\text{C}}$ is the pseudoequilibrium concentration of A·B achieved at 4 °C in the experimental premixing time range, $t_{4^\circ\text{C}}$ is the premixing time at 4 °C, and $\tau_{4^\circ\text{C}}$ is the characteristic time of mixing at 4 °C.

Symmetric Self-Dimer Model. The kinetic equations for the symmetric self-dimer model (Scheme 1) are utilized in fitting the titration experiments. The concentration of the heterologous dimer is given by

$$[\text{A}\cdot\text{B}] = [\text{B}\cdot\text{A}] = \frac{[\text{A}]_0[\text{B}]_0}{2([\text{A}]_0 + [\text{B}]_0)}\left[1 - \frac{K(-1 + \sqrt{1 + (8/K)([\text{A}]_0 + [\text{B}]_0)})}{4([A]_0 + [B]_0)}\right]$$

where K is the dissociation constant. The rate of mutant complementation, ν, is given by $\nu = k_{\text{cat}[\text{A}\cdot\text{B}]}([\text{A}\cdot\text{B}] + [\text{B}\cdot\text{A}]) = 2k_{\text{cat}[\text{A}\cdot\text{B}]}[\text{A}\cdot\text{B}]$. To correct for the possibility that one of the mutant samples is relatively more pure than the other, the scaling parameter α is introduced such that $[\text{A}]_0 = \alpha[\text{A}]_{0,\text{exp}}$ and $[\text{B}]_0 = \alpha^{-1}[\text{B}]_{0,\text{exp}}$, where $[\text{A}]_{0,\text{exp}}$ and $[\text{B}]_{0,\text{exp}}$ are the Bradford assay experimentally determined protein concentrations. To solve for the homogeneous dimer concentration in the concentration dependence of wild-type activity experiment, we have

$$[\text{WT}\cdot\text{WT}] = \frac{1}{K}\left(\frac{K}{4}\left[-1 + \sqrt{1 + \frac{8}{K}[\text{WT}]_0}\right]\right)^2$$

Inhibition Curve. The inhibition curve is used to fit the double-mutant inhibition titration experiment. In this experiment, the complementation activity of two mutants is inhibited by an increasing titer of a double mutant that is complementary to neither of the other two mutants. Let A and B represent the two complementary mutants and C represent the double mutant. The inhibition curve is given by relative rate $= 4[\text{A}]_0[\text{B}]_0/([\text{A}]_0 + [\text{B}]_0 + \delta[\text{C}]_0)^2$, where δ is a scaling parameter that relates the double-mutant concentration to its effective concentration as an inhibitor. The δ parameter is used to account for the possibility that the double mutant binds the single mutants more weakly than the two single mutants bind each other.

Gel Filtration. Gel-filtration chromatography was performed with a Sephadex 200 16/60 column, procedure as recommended by the manufacturer (Pharmacia Biotech). The running buffer contained 20 mM Tris, pH 7.5, 100 mM NaCl,

Scheme 2

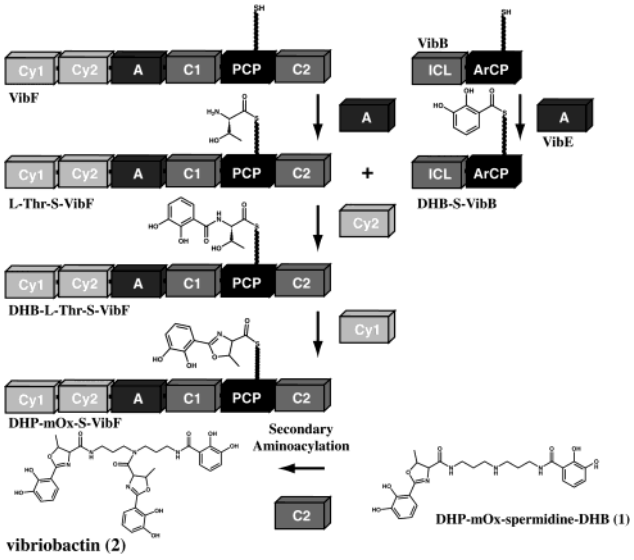

and 2 mM $MgCl_2$. The column was calibrated with thyroglobulin (669 kDa), ferritin (440 kDa), and catalase (232 kDa). The void volume was defined by the elution of blue dextran 2000 (2000 kDa). Each standard protein (5−10 mg) was dissolved in 1 mL of the running buffer, loaded on the column in a 250 μL volume at 0.5 mL/min, and eluted at the same flow rate. A 250 μL aliquot of 4.4 μM wild-type VibF was identically loaded and eluted.

Analytical Ultracentrifugation. Sedimentation equilibrium experiments were performed with a Beckman Optima XL-A. Equilibrium and Monte Carlo analyses were conducted with UltraScan version 5.0 (*20*). Hydrodynamic corrections for buffer conditions were made according to data published by Laue et al. (*21*), and the partial specific volume of VibF was estimated according to the method of Cohn and Edsall (*22*), as implemented in UltraScan. VibF samples were analyzed in buffer containing 20 mM Tris, pH 8, 50 mM NaCl, 2 mM $MgCl_2$, 1 mM dithiothreitol (DTT), and 10% glycerol at 4 °C at speeds ranging between 5000 and 12 500 rpm. Samples were spun in a 6-channel 12-mm external-fill equilibrium centerpiece in an An-60 Ti rotor. Scans (280 nm) were collected at equilibrium in radial step mode with 0.001 cm steps and 50 point averaging. Loading concentrations were 0.70, 0.40, and 0.25 OD, and data exceeding 0.9 OD were excluded. Data fitting was performed with a two-component model as implemented in UltraScan.

RESULTS

VibF Domain Mutants. The six-domain VibF subunit of the multicomponent vibriobactin synthetase carries out several enzymatic steps (*14*), from activation and autocatalytic loading of L-threonine as L-Thr-S-PCP, condensative transfer of a DHB moiety from DHB-S-ArCP held on the aryl carrier protein domain (ArCP) of VibB to produce DHB-L-Thr-S-PCP, and cyclodehydration to yield the dihydroxyphenyl-methyloxazolinyl (DHP-mOx)-S-PCP acyl enzyme form of VibF. This acyl group is transferred out to the primary amine of DHB-spermidine, freeing up VibF to go through another round of loading, condensation, and cyclodehydration to generate a second DHP-mOx-S-PCP. The last step in siderophore assembly is transfer of this DHP-mOx acyl group to the secondary amine of the norspermidine skeleton of compound **1**, just generated by the first DHP-mOx transfer, to produce vibriobactin **2** (Scheme 2). Assay of this last step, the acylation of the secondary amine position in the cosubstrate to produce vibriobactin, can be readily followed by HPLC analysis and requires all of the catalytic domains (Cy1, Cy2, A, and C2) of VibF to be functional, including the posttranslational conversion of S1891 in the PCP domain to the phosphopantetheinyl holo-VibF (*14*, *17*). The C1 domain has been shown by us previously (*14*) to be nonfunctional; it may serve as an architectural element or may be a remnant domain. Mutants were produced that, on the basis of bioinformatic and homology considerations (*14*, *17*, *19*), were expected to knock out activity of the Cy1 domain (Cy1*, a deletion, ΔCy1), the Cy2 domain (Cy2*, D595A), the A domain (A*, D1092A), the PCP domain by removing the side chain of the serine that must be phosphopantetheinylated (PCP*, S1891A), and the C2 domain (C2*, H2084A); see Chart 1. All these single-domain mutants were assayed in the secondary amine acylation assay that directly measures vibriobactin production by HPLC, with the des-DHP-mOx intermediate **1** as substrate along with ATP, threonine, and DHB. In addition, four types of double mutants of VibF were constructed: Cy1*Cy2* should be defective in both of the tandem Cy domains; Cy1*PCP* should knock out both Cy1 and PCP function in the same VibF polypeptide chain; Cy2*PCP* will abrogate Cy2 and PCP function within a VibF monomer; and A*PCP* analogously should take out A and PCP function within the same VibF molecule. Finally, a triple mutant, Cy1*Cy2*PCP*, should remove Cy1, Cy2, and PCP function within the same VibF protein molecules.

Table 1: VibF Adenylation Domain ATP−PP_i Exchange

VibF enzyme	k_{cat} (min^{-1})	K_m (mM)
wild type	1700 ± 34	0.6 ± 0.1
Cy1*	3900 ± 130	0.5 ± 0.1
Cy2*	670 ± 22	0.8 ± 0.1
A*	<8	*a*
PCP*	1500 ± 73	0.7 ± 0.1
C2*	1400 ± 74	1.1 ± 0.4
Cy1*Cy2*	890 ± 28	0.5 ± 0.1
Cy1*PCP*	610 ± 21	0.6 ± 0.1
Cy2*PCP*	990 ± 35	0.5 ± 0.1
A*PCP*	<24	*a*
Cy1*Cy2*PCP*	490 ± 17	0.6 ± 0.1

[a] Not determined.

ATP−PP_i Exchange Assay of VibF Mutants. As it was anticipated that many of the above mutant forms of VibF would be inactive in the vibriobactin formation assay, the L-Thr-dependent ATP−PP_i exchange activity, a measure of reversible formation of threonyl-AMP by the A-domain, was assayed to diagnose whether a mutation resulted in a global misfunction of the synthetase (Table 1). The rates for the two mutants containing the A* mutation, chosen to eliminate A-domain activity, were not significantly greater than the background exchange rate. This was the expected result, validating that the A-domain function had been lost, and this particular assay does not speak to the global function of these two mutants. The rates for the remainder of the mutants were comparable to those for wild type, with slightly lower values possibly indicating lower sample purity or long-range perturbations to A-domain activity. The K_m values for L-Thr

Table 2: VibF Secondary Aminoacylation Rates

VibF enzyme	rate (min^{-1})	% wild type	VibF enzyme pairs	rate (min^{-1})	% wild type
wild type	48	100	Cy1*+ PCP*	14.5	30.2
Cy1*	<0.5	<1.0	Cy1*+ Cy2*PCP*	7.0	14.6
Cy2*	0.7	1.4	Cy2* + PCP*	12.0	25.0
A*	<0.5	<1.0	Cy2* + C2*	10.6	22.1
PCP*	<0.5	<1.0	Cy2* + Cy1*PCP*	5.0	10.4
C2*	<0.5	<1.0	Cy2* + Cy2*PCP*	1.5	3.1
Cy1*Cy2*	<0.5	<1.0	Cy2* + A*PCP*	9.0	18.8
Cy1*PCP*	<0.5	<1.0	A* + Cy1*PCP*	7.4	15.5
Cy2*PCP*	<0.5	<1.0	A* + Cy2*PCP*	8.0	16.6
A*PCP*	<0.5	<1.0	A* + Cy1*Cy2*PCP*	5.4	11.2
Cy1*Cy2*PCP*	<0.5	<1.0	PCP* + C2*	2.3	4.8
detection limit	0.5	1.0	PCP* + Cy2*PCP*	0.6	1.3

Chart 2

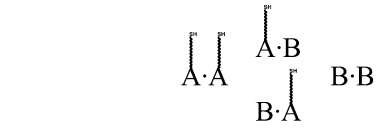

Population	25%	50%	25%
WT activity	0%	50%	0%
Net activity		25%	

recognition by these mutants were consistent with those of wild type.

*VibF Regain of Enzymatic Activity by Mutant Complementation in the Secondary Aminoacylation Assay, **1** → **2**.* The activity levels of the individual mutants are presented in the left-hand side of Table 2, in absolute turnover numbers in column 2 and as a percentage of wild-type VibF (48 min^{-1}) in column 3. With the exception of Cy2*, all mutants have activity levels less than the assay's detection limit (1% of wild type). The activity of Cy2* is only marginally above the detection limit and is small enough that this activity should not complicate the interpretation of the complementation experiments. These results establish that the deletion (Cy1) and the mutations (Cy2, A, PCP, C2) did indeed greatly compromise the function of the indicated domains of VibF. The residual activity levels of the individual mutants are sufficiently low to provide enough dynamic range in activity regain assays observed for mixtures of two different mutants.

The activity levels of 1:1 mixtures of different pairs of mutants are also listed in Table 2. The turnover (rates per minute) values in the fifth column are defined by the rate of vibriobactin production divided by the total concentration of the pairs of VibF enzymes. The first general observation is that, for several distinct mutant pairs, activity regain is detected and the vibriobactin formation rate is close to 25% of the wild-type rate, after the mutants were premixed for an hour at 30 °C. Given the assay conditions, this 25% value approaches the upper limit expected if VibF is active as a dimer. As a simplified heuristic to quickly arrive at the 25% value, consider Chart 2. Let A and B be two distinct complementary VibF mutants that are individually incompetent for secondary aminoacylation activity. Allow A to retain its capacity for PCP domain phosphopantetheinylation but force B to contain the PCP* mutation. If the two mutants are mixed in a 1:1 fashion, such that population is randomly scrambled, heterodimers should account for 50% of the species. The mutant homodimers are inactive, and the heterodimers are only half as active as wild-type homodimers, because the A/B pair only contains one tethered-intermediate attachment point (which effectively cuts output by half). The net result is that the activity regain should approach 25%, for half the population is half as active as wild type. The result that activity regain was detected close to this 25% value indicates that, unlike the DEBS PKS and animal FAS systems (*7*, *8*), where an additional anion-exchange chromatography step of domain mutants was necessary to quickly separate dimers into monomers so they could then reassociate, the monomer−oligomer forms of this NRPS module are in equilibrium under the assay conditions.

Scheme 3

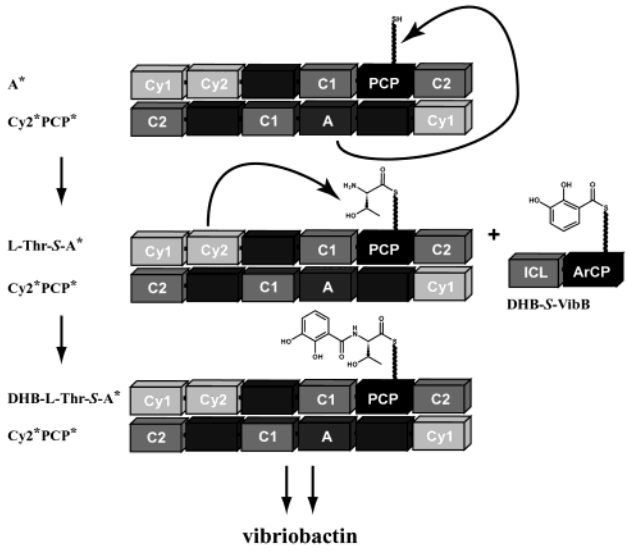

An example of productive secondary aminoacylation complementation to yield vibriobactin is given in Scheme 3. A* and Cy2* PCP* are mixed together, and a fraction of the total population comes together as a A*/Cy2*PCP* heterodimer (the presented hypothetical head-to-tail topology is only one of many possible dimer arrangements). This heterodimer has only one operational pantetheine arm (located on the PCP domain of A*) on which to covalently attach synthetic intermediates. The A-domain of A* is inactive, so the A-domain of Cy2*PCP* is forced to activate L-Thr and operate in trans on the neighbor chain's (A*'s) PCP domain to form the thioester, yielding L-Thr-S-A*/Cy2*PCP*. The Cy2 domain of Cy2*PCP* is inactive, so the Cy2 domain of A* must operate in cis on its own chain's PCP domain, catalyzing the condensation step between DHB-S-VibB and L-Thr-S-A* to yield DHB-L-Thr-S-A*/Cy2*PCP*. The Cy1 and C2 domains on both chains are operational, and a subset of these domains will proceed through the latter steps to produce vibriobactin.

The next general result is that pairs of intentionally noncomplementary mutants serve as lower limits for the positive pairs. The pairs that fail to give signals are those in which both copies of a domain are abrogated: the Cy2 domain in the Cy2*/Cy2*PCP* pair and the PCP domain in the PCP*/Cy2*PCP* pair. The rates of Cy2*/Cy2*PCP* and PCP*/Cy2*PCP* are 3.13% and 1.31% (respectively) of wild type, close to the detection limit of the assay.

The next result of note is that the A-domain mutation (A*) does not extensively perturb function, as Cy1, Cy2 and PCP

domains remain active (evidenced by the successful complementation of A* with Cy1*Cy2*PCP*). The other A-domain mutant, A*PCP*, appears similarly unaffected (the Cy2*/A*PCP* pair shows positive complementation).

Progressing to more domain-specific results, the Cy1, Cy2, and A domains can function for cyclodehydration or aminoacylation chemistry with PCP domains in the same chain in cis or on PCP domains on VibF molecules in trans. Both a Cy1 deletion and a Cy2 inactivating point mutation can be rescued by the corresponding domains on a VibF molecule whose PCP domain is nonfunctional, so Cy1 and Cy2 can service a threonyl-S-PCP intermediate in trans. The complementation rates of the Cy1*/PCP* and Cy2*/PCP* mutant pairs are 25−30% of the wild-type VibF turnover rates. When a mutation in an additional domain is introduced, as in Cy2*PCP* mixed with Cy1*, A*PCP* mixed with Cy2*, or Cy1*PCP* mixed with Cy2*, the observed reconstitution rates are lower. The average rate for the Cy1*/PCP* and Cy2*/PCP* mutant pairs is 27.6% of wild type vs 14.5% for the latter set of pairs (negative controls excluded). If the Cy1*/PCP* and Cy2*/PCP* mutant pairs are withheld, the difference in average complementation rate for the active Cy1, Cy2, or A domain with the same-chain PCP domain vs the neighbor-chain PCP domain is less than a factor of 1.4. That is, the Cy1, Cy2, and A domains have no substantial preference for either PCP domain. The Cy1*/PCP* mutant pair result pushes the Cy1 domain average in favor of the neighbor-chain PCP domain utilization to a factor of 1.8. The Cy2*/PCP* pair similarly affects the Cy2 domain, but the preference for the neighbor chain PCP remains small at a factor of 1.3.

In contrast, the difference in rate between the active C2 domain using either PCP domain (Cy2*/C2*) vs solely the neighbor-chain PCP domain (PCP*/C2*) is 4.6-fold. This implies that the C2 domain prefers to use the same-chain PCP domain by at least a factor of 3.6 to using the neighbor-chain PCP domain. The background complementation (negative control) rates are significant fractions of the observed rate for the PCP*/C2* pair, and this gives further perspective on the relative inefficiency of the C2 domain for using the neighbor-chain PCP domain in trans.

The two VibF Cy domains (Cy1 and Cy2) in tandem perform the cyclization step (*14*) normally executed in other NRPS assembly lines by a single Cy domain (*11*, *12*, *23*). In addition to individually testing Cy1 and Cy2 for compatibility with the same-chain and/or neighbor-chain PCP domain, it is important to evaluate the complementation activity when the active Cy domains are forced to reside side-by-side on the same chain or are separated onto opposite chains. If the Cy1/Cy2 domains fold into a conformation such that their active sites are spatially proximal, as their tandem operation might suggest, it is likely that the active Cy1 domain would be preferentially complementary to an active Cy2 domain either on the same chain or on the neighbor chain. This Cy domain logic may be contextually dependent on the location of the active PCP domain, and this possibility needs to be investigated as well. The complementation results in fact show that the active Cy1 domain has no preference for location of the active Cy2 domain. The activities are not significantly different for opposite-chain (Cy1*/Cy2*PCP* and Cy2*/Cy1*PCP*) vs same-chain (A*/Cy1*Cy2*PCP*) active Cy1/Cy2 domain combinations, and the opposite-chain combinations are not considerably contextually dependent on the location of the active PCP domain (Cy1*/Cy2*PCP* vs Cy2*/Cy1*PCP*).

Time Course for Regain of Catalytic Activity by Pairs of VibF Mutants. With the initial result of various VibF mutant protein activity complementations successfully established, several complementary pairs were studied further. To discriminate between transient in trans interactions in rapid on/off equilibrium and multiple turnovers arising from a long-lived dimer, vibriobactin formation initial velocity rates were measured as a function of premixing time before the 3-min activity assay at 30 °C. In the limit of transient complementation, the rates of complex formation (k_{on}) and dissolution (k_{off}) should occur faster than a single turnover, or about 50 times per minute at 30 °C. Since the transient formation/dissociation rate is much faster than the 3-min assay time, there should be no premixing time dependence if transient complementation is the proper model. On the other hand, if the formation/dissociation rate were slower than the assay time, then one would expect the complementation activity to increase and eventually plateau with increasing times of premixing before assay. This would be the case, for example, in the dimeric complementation model, with a dimer partner exchange rate slower than 3 min at 30 °C.

In the case of multiple-turnover complementation, premixing time experiments are additionally useful for optimizing conditions for heterologous dimer formation. While the results from the mutant complementation assays establish that a 1-h premixing time at 30 °C is sufficient to achieve the expected wild-type rate fraction, it is feasible that premixing for a shorter time, or at a lower temperature, would be preferable. In the animal FAS system, the dimer pairs are cold-labile (dissociate more rapidly at lower temperatures), and reassociation is promoted at increased temperatures (*7*). If this were to hold true for the VibF system, it would be advisable to premix at 4 °C for the prerequisite time and then perform the activity assay at 30 °C.

The premixing time results for the Cy2*/PCP* (Figure 2A) and Cy2*/C2* (Figure 2B) pairs support the dimer complementation model. For the Cy2*/PCP* pair, the fit to the exponential equilibration model results in a $2k_{cat[A\cdot B]}[A\cdot B]_{eq}$ value of 3.6 ± 0.7 μM min^{-1}, a τ of 56 ± 17 min, an $[A\cdot B]_{eq}^{4°C}/[A\cdot B]_{eq}$ value of 7.4% ± 0.2%, and a $\tau_{4°C}$ of 0.8 ± 0.1 min. The first observation is that the vibriobactin synthesis activity increases with the premixing time at 30 °C and the characteristic time for this increase is much longer, by up to 3 orders of magnitude, than a single catalytic turnover. The next observation is that the pseudoequilibrium concentration of heterologous dimer achieved during the premixing at 4 °C is significantly less than the analogous concentration achieved during the premixing at 30 °C. Furthermore, the characteristic time to achieve the pseudoequilibrium at 4 °C is much faster than that at 30 °C. These results indicate that VibF dimer pairs are not especially cold-labile and that it is not preferable to premix mutants at 4 °C before assay.

For the Cy2*/C2* pair, the fit to the exponential equilibration model results in a $2k_{cat[A\cdot B]}[A\cdot B]_{eq}$ value of 2.1 ± 0.2 μM min^{-1} and a τ of 14 ± 4 min. As was the case for the Cy2*/PCP* pair, the vibriobactin synthesis activity increases with the premixing time at 30 °C, and the characteristic time is at least 100-fold longer than a single catalytic turnover.

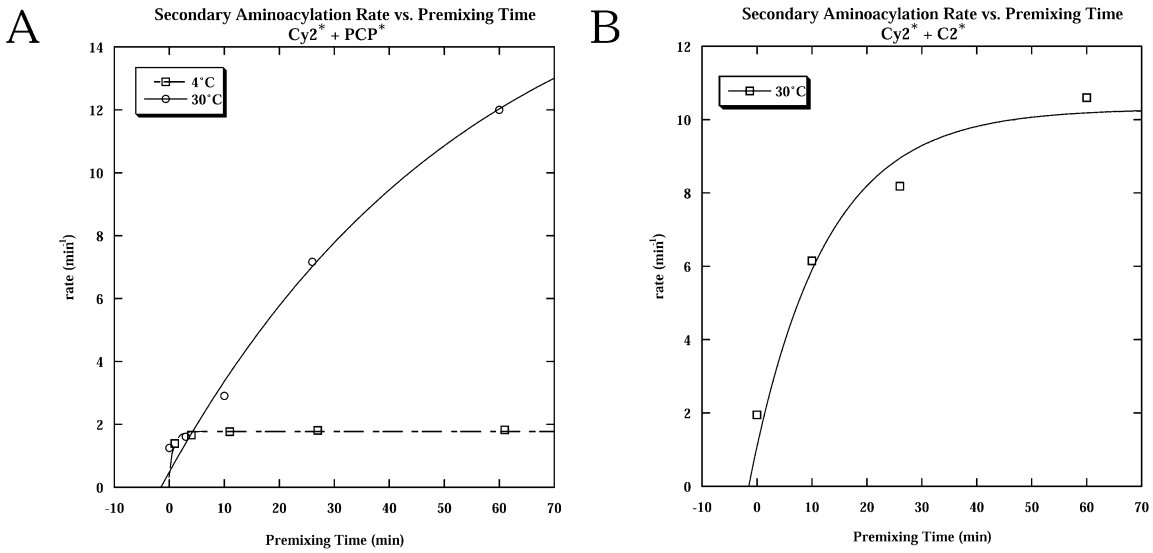

FIGURE 2: Premixing time experiments: (A) 100 nM Cy2* and 100 nM PCP* premixed at either 4 or 30 °C before the secondary amine acylation assay; (B) 100 nM Cy2* and 100 nM C2* premixed at 30 °C before assay. Solid and dashed lines are the exponential equilibration best fits to the data.

The shorter characteristic time for the Cy2*/C2* pair makes the rate plateau more apparent. The results from both mutant pairs suggest that premixing at 30 °C for 1 h is reasonable to obtain near-equilibrium heterologous dimer formation and maximal complementation activity and support the comparison data in Table 2.

Concentration Dependence of VibF Activity and Titration Experiments with Single Mutants. As a point of reference for titration experiments of mutant VibF proteins in activity regain assays, the vibriobactin synthetase activity of wild-type VibF was assayed as a function of the enzyme concentration, from 20 to 500 nM. In the symmetric self-dimer model for mutant complementation, production of vibriobactin only occurs in the context of two heterologous complementary VibF mutants forming a dimeric pair, because neither mutant is individually competent. There is no such a priori requirement for wild-type VibF, because both monomeric and dimeric forms have all the prerequisite operational modules. However, if the assumption is made that the wild-type activity also occurs only in the dimeric state, the best-fit curve (see Experimental Procedures; data not shown) results in a dissociation constant K of 41 nM, and a k_{cat} of 62 min^{-1}. This k_{cat} value is based on the concentration of dimer tethered-intermediate attachment points, or equivalently 2 times the dimer concentration (because there are two attachment points per wild-type dimer). This contrasts with the wild-type value presented in the second column of Table 2, which is defined by the production rate divided by the total enzyme (monomer plus dimer) concentration.

In the parallel enzyme titration experiment, the activity of a 1:1 mixture of Cy2* and C2* was assayed as a function of the total mixed enzyme concentration, from 50 to 400 nM. The best-fit curve (data not shown) resulted in a dissociation constant K of 50 nM and a k_{cat} of 62 min^{-1}. This k_{cat} value is based on the effective concentration of heterologous mutant dimer tethered-intermediate attachment points, or equivalently the heterologous dimer concentration (one effective attachment point per Cy2*/C2* pair because the residually active C2 domain has a strong preference for its same-chain PCP domain). The dimer dissociation constant and the catalytic rate for the Cy2*/C2* pair in this experiment agree well with the corresponding values for wild type.

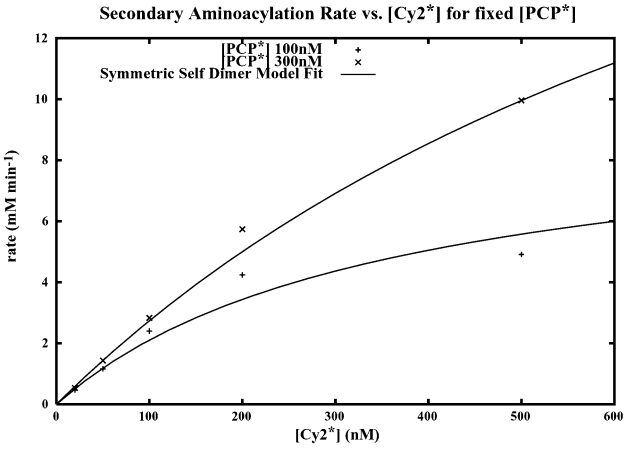

FIGURE 3: Titration experiment. The concentration of PCP* is fixed at either 100 or 300 nM, and the secondary amine acylation rate is assayed as a function of the concentration of Cy2*. Solid lines are the symmetric self-dimer model's best fit to the data.

To further evaluate the symmetric self-dimer model, the catalytic activity of a mixture of Cy2* and PCP* was assayed as a function of varying Cy2* concentration, holding the concentration of PCP* fixed at either 100 or 300 nM (Figure 3). The symmetric self-dimer model's best fit to the data resulted in a dissociation constant K of 22 nM, a k_{cat} of 60 min^{-1}, and a relative concentration scaling factor α of 0.6 in favor of the PCP* mutant. This k_{cat} value is based on the concentration of heterologous mutant dimer tethered-intermediate attachment points, or equivalently the heterologous dimer concentration (as it is defined in the Experimental Procedures section). The dissociation constant and catalytic rate for the Cy2*/PCP* pair agree well with the corresponding Cy2*/C2* pair and wild-type values. The concentration scaling factor α, indicating that the sample purity of active PCP* is relatively higher than that of active Cy2*, is in agreement with the results of the ATP−PP$_i$ exchange assay for the two mutants.

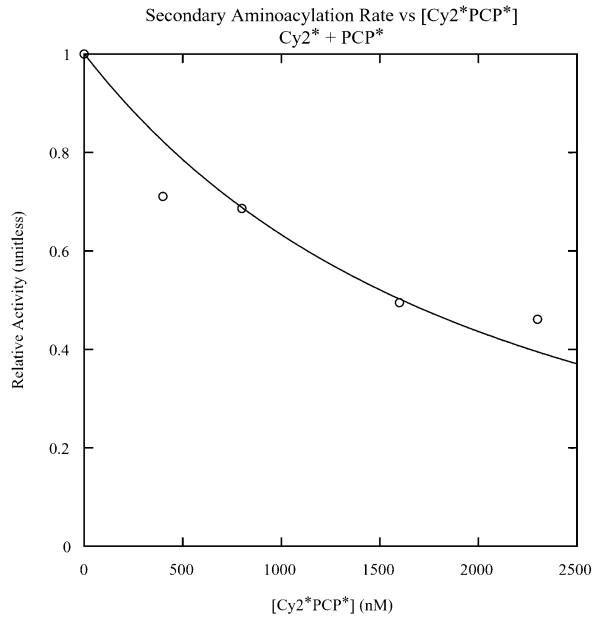

FIGURE 4: Double-mutant titration experiment. The relative secondary amine acylation activity of 400 nM Cy2* and 400 nM PCP* is assayed as a function of the concentration of the double mutant Cy2*PCP*. The solid line is the dominant negative inhibition curve best fit to the data.

Double-Mutant Inhibition Titration. The symmetric self-dimer model predicts that a VibF double mutant should inhibit complementation activity when the double mutant contains both of the mutations found within the complementary pair. To test this prediction, the secondary aminoacylation activity of the Cy2*/PCP* pair was assayed in the presence of increasing amounts of the double mutant Cy2*PCP* concentration (Figure 4). The observed vibriobactin synthetase activity decayed with increasing titer of the double mutant. The inhibition curve best fit results in a δ of 0.21 $\pm$ 0.03, indicating that Cy2*PCP* is not as effective an inhibitor as anticipated (around a δ of 1.0). The smaller δ is likely due to the double mutant binding the single mutants more weakly than the two single mutants bind each other. The positive complementation result between A* and Cy2*PCP* displayed in Table 2 dispels the notion that Cy2*PCP* is simply misfolded, or not operating properly, as an explanation for the observed δ.

Gel Filtration and Sedimentation Equilibrium Analytical Ultracentrifugation of Wild-Type VibF. To complement the biochemical studies, gel filtration and analytical ultracentrifugation were utilized as physical measurements to determine the oligomeric state of wild-type VibF. In the gel-filtration experiment, VibF (271 kDa) eluted in two post-void volume peaks, corresponding to estimated molecular masses of 715 and 445 kDa. It is assumed that these peaks represent nonglobular dimer and monomer, and such inflated apparent weights have previously been observed for the yersiniabactin synthetase NRPS−PKS hybrid enzyme HMWP1 (*9*). The two peak sizes were comparable, with the integrated area suggesting a 2−3-fold preference for the higher molecular weight peak under the gel-filtration conditions. Fractions representative of the two peaks were electrophoresed side by side in SDS−PAGE (Figure 5), and both of these fractions had wild-type levels of catalytic activity (data not shown). It should also be noted that the small

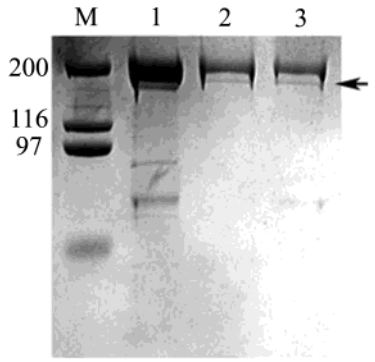

FIGURE 5: SDS−10% PAGE of 271 kDa VibFWT. M, molecular weight standards. Lane 1, sample used in gel-filtration and analytical ultracentrifugation experiments; lane 2, gel-filtration fraction corresponding to 715 kDa peak; lane 3, gel-filtration fraction corresponding to 445 kDa. Arrow at right points to the approximately 160 kDa degradation product observed in all three lanes.

amount of protein degradation product around 160 kDa in the VibF sample used for the gel filtration and sedimentation equilibrium experiments was retained in both of the peak representative fractions.

To further establish the association properties of wild-type VibF, sedimentation equilibrium experiments were conducted at several protein concentrations (Figure 6). For the global equilibrium analysis, nine scans (Figure 6A) of speeds ranging from 5000 to 12 500 rpm and 0.70, 0.40, and 0.25 OD (2.04, 1.16, and 0.73 μM) loading concentrations were fit to a two-component model. The two-component model was applied to account for the presence of the lower mass degradation product (Figure 5) as well as for the full-length VibF species. The degradation product and full-length VibF molecular weights were floated global parameters and were forced to be the same for all the included data sets. The system could be well described with this model, which resulted in random residuals (Figure 6B) and a VibF molecular mass of 544.5 $\pm$ 13.8 kDa, which is in agreement with the protein sequence predicted dimer molecular mass (541.9 kDa). The degradation product molecular mass of 144.0 $\pm$ 7.4 kDa is in agreement with the SDS−PAGE estimated mass of 160 $\pm$ 25 kDa. In all fitted scans, the degradation product accounted for less than 6% of the optical density above baseline and is only significant (greater than 1% of the optical density) in the higher speed scans of the highest loading concentration. This observation agrees with the relative staining of the two SDS−PAGE bands.

The data fitting did not significantly improve with a three-component model, where the final component was added to account for the presence of monomeric full-length VibF. The necessity of including the degradation product component in the fit prevented the use of the monomer−dimer model (which results in nonrandom/systematic residuals), and consequentially the sedimentation equilibrium analysis was unable to establish the dissociation constant for the system.

DISCUSSION

With all four vibriobactin synthetase proteins purified and fully reconstituted to give robust activity for siderophore synthesis, we have produced inactivating mutants and/or deletions in various domains of VibF to ascertain their respective functions (*14*). In the course of evaluating the

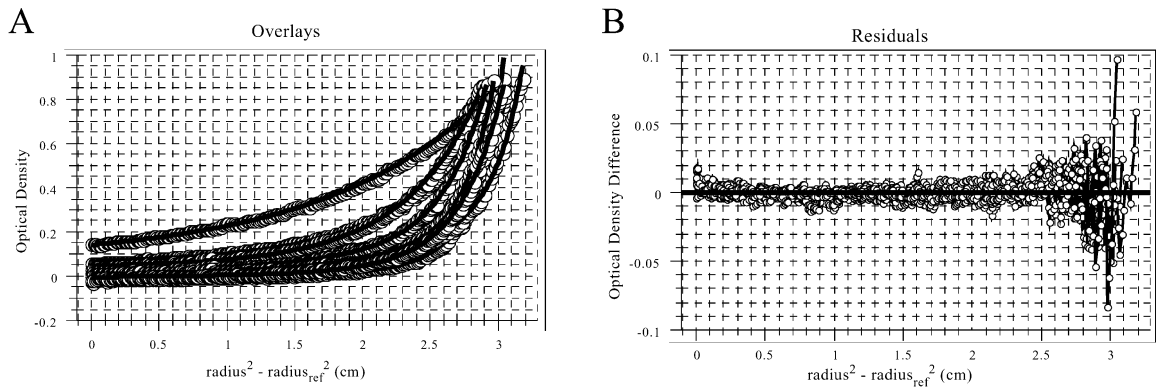

FIGURE 6: Sedimentation equilibrium analytical ultracentrifugation analysis of VibFWT: (A) overlay of nine wavelength scans and (B) residuals from the global fit of the data as described under Experimental Procedures.

inactive mutant forms of VibF, we analyzed whether pairs of inactive mutants, when mixed together, could restore activity. The results reported in this paper establish several such functional complementations, place constraints on active oligomeric states of VibF, and allow comparison to other NRPS, PKS, and FAS assembly line oligomer states.

From the initial indications that phosphopantetheine was the prosthetic group for the carrier protein domains, first in fatty acid synthases and then in polyketide synthases, the molecular logic of covalent tethering of acyl enzyme intermediates during chain elongation steps by FAS and PKS assembly lines became understood. NRPS responsible for the construction of both peptides and siderophores are comprised of multidomain modules, each with an embedded phosphopantetheinylated carrier protein domain, extending the parallels in assembly line organization. In general the FAS assembly lines are simplified in comparison to PKS and NRPS in both modularity and content of optional domains. FAS contains one seven-domain module per subunit, while the three subunits, DEBS1, 2, and 3, in deoxyerythronolide biogenesis each are bimodular. Tyrocidine synthetase has 10 modules distributed over three subunits, TycA, B, and C, with TycC containing six modules. The 11-module cyclosporin synthetase has them all in a single 1.6 MDa subunit. In multimodular subunits the likely path for transfer of elongating acyl chain between modules is in cis. However, previous data on FAS and the DEBS PKS subunits have indicated they are homodimers, the monomers are inactive, and catalytic domains on one subunit can service acyl-S-ACP chains on an adjacent subunit in the homodimer (*5*, *6*); that is, some catalytic functions can work in trans. These observations of in trans functions have been dissected in FAS dimers by disassociation of homodimers inactivated in a particular domain (KS or ACP), reassociation of mixed pairs of mutants, and measuring regain of FAS activity. In turn, these results on molecular complementation have led to models for the orientation of domains within FAS and PKS dimers, as shown in Figure 1B.

When NRPS assembly lines were probed for comparable formation of stable oligomers, e.g., module/subunit homodimers, no evidence had been forthcoming that species other than monomer forms were active (*9*). The results described here with VibF are the first indication in an NRPS module that such homodimerization can occur and indicate there can be a continuum of functional oligomerization states between monomers and dimers in nonribosomal peptide synthetases. This may be of particular relevance in understanding how PKS/NRPS hybrids interact, as in the epothilone synthase, where EpoA and EpoC are PKS modules and expected to be dimeric while EpoB is an NRPS module that is acceptor for EpoA and donor for EpoC (*23*). VibF is a nontraditional NRPS in both domain organization and iterative transfer of its tethered intermediate. It would be interesting to observe nonmonomeric active states for other nontypical NRPS systems.

The reconstitution of VibF activity from Cy1, Cy2, A, PCP, and C2 mutants behave in an internally consistent manner for dimer formation. The mutant pairs with tandem mutations in PCP or Cy2 domains behave appropriately as nulls since neither VibF component in a dimer can provide the required carrier (PCP) or catalytic (Cy2) domain, and the double mutant with dual PCP and Cy2 domain mutations operates as an inhibitor of complementation between PCP and Cy2 domain single mutants. One-to-one mixtures of several mutant pairs give a regain of 25% of wild-type activity. The activity regain of a successfully complementing dimeric pair of mutants is also expected to be 25% of the wild-type level. This expectation makes several assumptions: (1) there is an equal amount of each mutant in the mixture, (2) the binding constants for the two homodimers and the heterodimer are about the same, (3) there is sufficient time/agitation to homogeneously mix the two mutants to achieve equilibrium, (4) the activity level of each individual mutant is essentially zero, and (5) the activity of the heterodimer is close to 50% that of a wild-type homodimer. The first condition is experimentally accessible. The binding constants of the homodimers and heterodimers are not tunable, but the extent of similarity between the best-fit dissociation constants for the wild type, Cy2*/C2*, and Cy2*/PCP* concentration dependence/titration experiments gives credibility to the second assumption. The time course for activity regain experiments suggest that the 1-h premixing time at 30 °C is reasonable to obtain near-equilibrium amounts of heterodimer formation. The low activity levels of the individual mutants comply with the fourth condition. The extent of agreement between the best-fit k_{cat} values (based on the effective concentration of tethered-intermediate points) for the wild type, Cy2*/C2*, and Cy2*/PCP* concentration dependence/titration experiments supports the notion that forcing one of the two mutants in the complementation pair to include the PCP mutation PCP* or the C2 mutation C2* satisfies the last condition. With all of the

above assumptions met, the upper limit approaching 25% wild-type activity regain is quite justified, and thus the observed activity regain is consistent with dimer formation. Gel-filtration data suggest dimer and monomer forms of VibF exist under the chromatographic conditions, and the ultracentrifugation studies suggest VibF dimers predominate at their analyzed loading concentrations. Given that the concentration of VibF eluting from the gel-filtration column was roughly 100 nM and that the ultracentrifuge loading concentrations ranged from 0.73 to 2.04 μM, these physical measurement results are consistent with a dissociation constant for VibF between 10 and 50 nM and thereby with the dissociation constants derived from the concentration dependence/titration experiments. The accrued evidence points to wild-type VibF dimers as the functional quaternary structure.

The regain of activity in pairs of mutant VibF proteins is slow on the experimental time scale and takes from 15 to 50 min at 30 °C, orders of magnitude longer than k_{cat} values for the last step of vibriobactin biosynthesis, at about 1 s^{-1}, so hundreds to thousands of catalytic cycles occur before dissociation of the mutant pairs of VibF. The VibF dimer dissociation/reassociation kinetics are different at 4 °C and it remains to be worked out whether temperature-dependent conformational changes are at work, but it is clear the pattern of VibF dissociation/reassociation is distinct from those of FAS and PKS dimers. whose mixing at 30 °C is inefficient for subunit exchange. The result that only a pseudoequilibrium of VibF heterodimer is achieved at 4 °C, and that the fully scrambled equilibrium concentration is not obtained, indicates that the rate-limiting step to total equilibration at cold temperatures is longer than the time scale of the premixing course. This rate-limiting step is likely the dissociation of homodimers (as source of monomers for subsequent heteroassociation), implying that the characteristic time to pseudoequilibration at 4 °C is describing the association rate of monomers to yield complementary heterodimers.

Given the evidence for functional dimers reconstituted from inactive VibF mutant pairs, the activity levels from particular pairs allow some conclusions to be drawn. The two condensation/cyclodehydration domains Cy1 and Cy2 can act equally well to transfer a DHB moiety onto a threonyl-S-PCP in the same or adjacent VibF subunit. Likewise the A domain can make threonyl-AMP and then load it as the threonyl-S-PCP covalent intermediate equally well when it is in cis or in trans to the PCP domain. It is not yet known if this reflects a symmetrical architectural positioning of Cy1, Cy2, and A relative to the PCP domains in VibF dimers and/or that none of those chemical steps is rate-determining in vibriobactin formation. If these steps are fast relative to an overall slow step, then any diminution in elementary rate constants due to mispositioning of domains that now have to act in trans would be suppressed by the subsequent slow step. By contrast, the C2 domain has about a 3−4-fold preference for using the in cis DHP-mOx acyl chain over the in trans partner as electrophilic donor to the DHP-mOx-spermidine-DHB nucleophilic cosubstrate **1**. Again, this could be an architectural asymmetry in the VibF dimer and/or the C2-mediated amide bond formation could be the rate-determining step. Nor is it yet clear why accrual of multiple mutations in a VibF module slows down k_{cat}, although multiplicative reductions in rates of elementary steps could be the answer. Further delineation of how C, A, and Cy domains of the VibF NRPS module can act efficiently in trans should shed light on the natural in trans chain transfers across subunit interfaces in multisubunit assembly lines, e.g., in tyrocidine and vancomycin synthetases (*3*, *4*). That information may have lessons for engineering of NRPS/PKS junctions, where dimer/monomer oligomeric states may be of consequence. Elucidation of which domains of VibF contribute to homodimer stability and functional orientation for in trans interaction of catalytic and carrier protein domains may likewise be of general utility for controlling oligomeric states of other NRPS modules in natural product assembly lines.

ACKNOWLEDGMENT

We thank Jeff Cruzan and Susanne Swalley for technical assistance in setting up the analytical ultracentrifugation experiments and Steven Bruner, C. Gary Marshall, and Stephan Sieber for reading of the manuscript.

REFERENCES

1. Smith, S. (1994) *FASEB J. 8*, 1248−59.
2. Cane, D. E., and Walsh, C. T. (1999) *Chem. Biol. 6*, R319−R325.
3. Marahiel, M. A., Stachelhaus, T., and Mootz, H. D. (1997) *Chem. Rev. 97*, 2651−2673.
4. Pootoolal, J., Thomas, M. G., Marshall, C. G., Neu, J. M., Hubbard, B. K., Walsh, C. T., and Wright, G. D. (2002) *Proc. Natl. Acad. Sci. U.S.A. 99*, 8962−8967.
5. Staunton, J., Caffrey, P., Aparicio, J. F., Roberts, G. A., Bethell, S. S., and Leadlay, P. F. (1996) *Nat. Struct. Biol. 3*, 188−192.
6. Joshi, A. K., Witkowski, A., and Smith, S. (1998) *Biochemistry 37*, 2515−2523.
7. Witkowski, A., Joshi, A., and Smith, S. (1996) *Biochemistry 35*, 10569−10575.
8. Kao, C. M., Pieper, R., Cane, D. E., and Khosla, C. (1996) *Biochemistry 35*, 12363−12368.
9. Sieber, S. A., Linne, U., Hillson, N. J., Roche, E., Walsh, C. T., and Marahiel, M. A. (2002) *Chem. Biol. 9*, 997−1008.
10. Patel, H. M., and Walsh, C. T. (2001) *Biochemistry 40*, 9023−9031.
11. Quadri, L. E. N., Keating, T. A., Patel, H. M., and Walsh, C. T. (1999) *Biochemistry 38*, 14941−14954.
12. Miller, D. A., Luo, L., Hillson, N., Keating, T. A., and Walsh, C. T. (2002) *Chem. Biol. 9*, 333−344.
13. Keating, T. A. M., Gary, C., and Walsh, C. T. (2000) *Biochemistry 39*, 15522−15530.
14. Marshall, C. G., Hillson, N. J., and Walsh, C. T. (2002) *Biochemistry 41*, 244−250.
15. Henderson, D. P., and Payne, S. M. (1994) *Infect. Immun. 62*, 5120−5125.
16. Griffiths, G. L., Sigel, S. P., Payne, S. M., and Neilands, J. B. (1984) *J. Biol. Chem. 259*, 383−385.
17. Marshall, C. G., Burkart, M. D., Keating, T. A., and Walsh, C. T. (2001) *Biochemistry 40*, 10655−10663.
18. Sambrook, J., Fritsch, E. F., and Maniatis, T. (1989) *Molecular Cloning: A Laboratory Manual*, 2nd ed., Cold Spring Harbor Press, Plainview, NY.
19. Stachelhaus, T., Mootz, H. D., and Marahiel, M. A. (1999) *Chem. Biol. 6*, 493−505.
20. Lambert, L. J., Schirf, V., Demeler, B., Cadene, M., and Werner, M. H. (2001) *EMBO J. 20*, 7149−59.
21. Laue, T. M., Shah, B. D., Ridgeway, T. M., and Pelletier, S. L. (1992) in *Analytical ultracentrifugation in biochemistry and polymer science* (Harding, S. E., Rowe, A. J., and Horton, J. C., Eds.) pp 90−125, Royal Society of Chemistry, Cambridge, U.K.
22. Cohn, E. J., and Edsall, J. T. (1943) *Proteins, Amino Acids and Peptides as Ions and Dipolar Ions*, Reinhold, New York.
23. O'Connor, S. E., Chen, H., and Walsh C. T. (2002) *Biochemistry 41*, 5685−94.
24. Rangan, V. S., Joshi, A. K., and Smith, S. (2001) *Biochemistry 40*, 10792−10799.

BI026903H